Performance Analysis of AoA Estimation under Hardware Impairments in a RIS-assisted MIMO System

Hyunsoo Lee, Adam Dubs, and Sunwoo Kim
Department of Electronic Engineering, Hanyang University, Seoul, South Korea
{geniusoo, duanandi16, remero}@hanyang.ac.kr

Abstract

This paper investigates the performance of angle-of-arrival (AoA) estimation under hardware impairments in a reconfigurable intelligent surface (RIS)-assisted millimeter-wave (mmWave) multiple-input multiple-output system. The AoA can be estimated by the coarse angle through measuring power on permissible incident regions. The investigated algorithm shows the enhanced potential in terms of hardware implementation feasibility, such as lower computational complexity than the maximum likelihood.

***Index Terms*—Reconfigurable intelligent surface, sensing, MIMO**

I. Introduction

Reconfigurable intelligent surface (RIS) has been focused as a pivotal technology whereby its surfaces are endowed with the capability to actively modify the impinging electromagnetic wave [1]. Furthermore, the RIS can provide obvious benefits in terms of communication, positioning, and sensing by leveraging intended reflection [2], [3]. However, a critical challenge is to compensate the hardware impairments. For instance, the unconcerned hardware impairments affects as a bias for the range and angle estimation, even all components are synchronized.

To that end, this paper investigates a focal scanning (FS) to estimate angle-of-arrival (AoA) for RIS-assisted millimeter-wave (mmWave) communication system under hardware impairments and multipath propagation. By measuring the received power over the distance and beam direction at the RIS, the AoA is estimated by the FS method with lower computational complexity compared to the maximum likelihood (ML) method. The simulation results provide insights for deploying RIS-assisted system for mmWave communication.

II. System Model

This paper considers single-user orthogonal frequency division multiplexing (OFDM) mmWave multiple-input multiple-output (MIMO) system in uplink scenario, as shown in Fig.1. Note that an user equipment (UE) and a base station (BS) employ analog beamforming structure, where the UE and BS are equipped with M_U and M_B uniform planar arrays (UPAs) with half-wavelength spacing $\lambda/2$, respectively. Here, the RIS equipped with M_R antenna elements reflects the UE signal to the BS.

The UE-to-RIS channel with the number of L_UR can be given by

$$\mathbf{H}_\mathrm{UR} = \sum_{l=1}^{L_\mathrm{UR}} \alpha_\mathrm{UR}^l \mathbf{a}(\phi_\mathrm{UR}^l)\mathbf{a}(\theta_\mathrm{UR}^l)^\mathsf{H} \in \mathbb{C}^{M_\mathrm{R}\times M_\mathrm{U}}, \tag{1}$$

where α_UR^l, $\mathbf{a}(\phi_\mathrm{UR}^l)$, and $\mathbf{a}(\theta_\mathrm{UR}^l)$ respectively denote the channel gain, the UE-to-RIS AoA, and the UE-to-RIS angle-of-departure (AoD) of the l-th path.

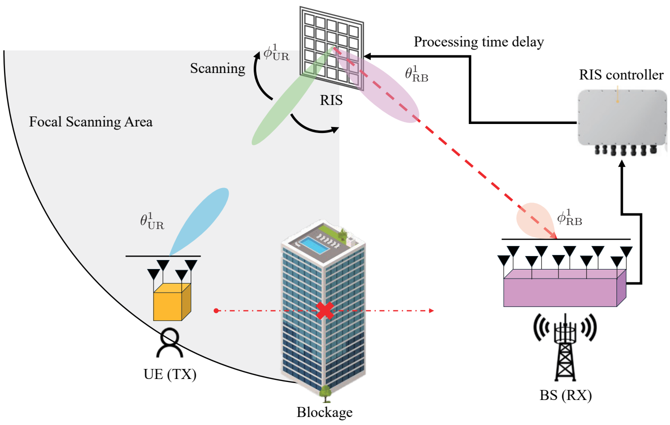

Fig. 1: A sensing scheme of uplink RIS-assisted mmWave MIMO system and propagation paths.

Unlike the UE-to-RIS channel, there is only one RIS-to-BS channel, $\mathbf{H}_\mathrm{RB}$, can be given by

$$\mathbf{H}_\mathrm{RB} = \sum_{l=1}^{L_\mathrm{RB}} \alpha_\mathrm{RB}^l \mathbf{a}(\phi_\mathrm{RB}^l)\mathbf{a}(\theta_\mathrm{RB}^l)^\mathsf{H} \in \mathbb{C}^{M_\mathrm{B}\times M_\mathrm{R}}, \tag{2}$$

where L_RB denotes the number of signal paths between RIS and BS. Here, α_RB^l, $\mathbf{a}(\phi_\mathrm{RB}^l)$, and $\mathbf{a}(\theta_\mathrm{RB}^l)$ respectively denote the channel gain, the RIS-to-BS AoA, and the RIS-to-BS AoD of the l-th path. The BS controls the RIS, and the RIS control vector $\boldsymbol{\omega}$ can be given by

$$\boldsymbol{\omega} = \left[\beta_1 e^{j\vartheta_1}, \beta_2 e^{j\vartheta_2}, \ldots, \beta_{M_\mathrm{R}} e^{j\vartheta_{M_\mathrm{R}}}\right] \in \mathbb{C}^{M_\mathrm{R}\times 1}, \tag{3}$$

where β_m and ϑ_m denote a reflection coefficient and a phase shift of the m-th antenna in RIS, respectively.

The cascaded channel can be represent with the RIS control matrix $\boldsymbol{\Omega} = \mathrm{diag}(\boldsymbol{\omega})$,

$$\mathbf{H} = \mathbf{H}_\mathrm{RB}\boldsymbol{\Omega}\mathbf{H}_\mathrm{UR} \in \mathbb{C}^{M_\mathrm{B}\times M_\mathrm{U}}. \tag{4}$$

Here, the received signal with the BS combiner $\mathbf{w} \in \mathbb{C}^{M_\mathrm{B}\times 1}$ and UE precoder $\mathbf{f} \in \mathbb{C}^{N_\mathrm{U}\times 1}$ at time step t and k-th subcarrier

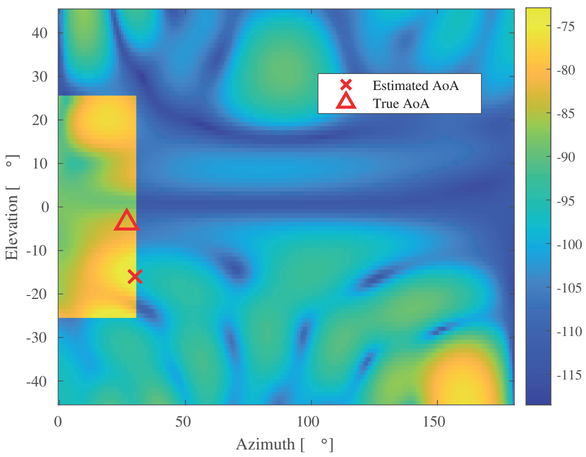

Fig. 2: The power spectrum and estimated azimuth and elevation of the UE, at the RIS.

can be represented as

$$y_{k,t} = \mathbf{w}_t^{\mathsf{H}} \mathbf{H} \mathbf{f}_t x_{k,t} + n_{k,t}$$
$$= \sum_{l=1}^{L_{\text{Tot}}} \alpha_l e^{-j2\pi(\tau_l+\tau_p)k\Delta f} e^{j2\pi t T_o} x_{k,t} + n_{k,t}, \qquad (5)$$

where $L_{\text{Tot}} = L_{\text{UR}} L_{\text{RB}}$. $\tau_l, \tau_p, \Delta f, T_o, n_{k,t}$ are the propagation delay, hardware processing time delay, the subcarrier spacing, the total OFDM symbol, and the additive Gaussian noise, respectively. Here, $\alpha_l = \alpha_{\text{UR}}^p \beta_{M_{\text{R}}} e^{j\vartheta_{M_{\text{R}}}} \alpha_{\text{RB}}^q$, and k-th subcarrier's phase offset φ_k is owing to the hardware processing time delay, $\varphi_k = -2\pi\Delta f(\tau_l + \tau_p)$.

III. Focal Scanning Method

The RIS-assisted system to estimate AoA carried out from the received signal assumes an imaginary focal point as the incident wave source. Note that the imaginary focal point is calculated from beam scanning within permissible incident region of the RIS.

Let $\boldsymbol{\omega}_t$ and Ξ denote the RIS control vector and the unknown position of the UE's UPA center $\Xi = (x_{\text{UE}}, y_{\text{UE}}, z_{\text{UE}})$. The distance between the UE and Ξ, d_{UR}, is assumed to be unknown. The log-likelihood function with hardware processing time delay is given by [4]

$$f(\{y_{k,t}\} \mid \Xi, \{\boldsymbol{\omega}_t\}, d_{\text{UR}}, \tau_p)$$
$$= -\frac{1}{\sigma^2} \sum_{t=1}^{T_o} \sum_{k=1}^{K} \left| y_{k,t} - \tilde{y}_{k,t}(\Xi; \boldsymbol{\omega}_t, d_{\text{UR}}, \tau_p) \right|^2, \qquad (6)$$

TABLE I: Simulation parameter configuration

Parameters	Value
Radio frequency	28 GHz
# of subcarrier (@bin spacing)	1000 (@480 kHz)
# of M_{U}, M_{R}, M_{B}	4×4, 32×32, 4×4
Azimuth field-of-view (@bin beam steering)	$0°$ to $180°$ (@3°)
Elevation field-of-view (@bin beam steering)	$-45°$ to $45°$ (@3°)

with the ML criterion

$$\hat{\Xi}, \hat{d}_{\text{UR}}, \hat{\tau}_p = \underset{\Xi, d_{\text{UR}}, \tau_p}{\arg\max}\, f(\{y_{k,t}\} \mid \Xi, \{\boldsymbol{\omega}_t\}, d_{\text{UR}}, \tau_p). \qquad (7)$$

Consider $\mathbf{p}_t$ denotes the location of the t-th imaginary focal point (or line) with the desired resolution for the FS method. From (7), the estimation of Ξ by the FS method without considering the number of angle and distance test points can be given by

$$\hat{\Xi} = \mathbf{p}_{\tilde{t}}, \quad \tilde{t} = \arg\max_t \sum_{t=1}^{T_o} \sum_{k=1}^{K} |y_{k,t}|^2. \qquad (8)$$

IV. Simulation Setup and Results

For the simulation setting, L_{UR} and L_{RB} are respectively set to 4 and 3. Here, the line-of-sight (LoS) path does not exist between the UE and BS, as shown in Fig. 1. However, the LoS path and diffused NLoS path do exist in UE-to-RIS and RIS-to-BS. The simulation parameter configuration in detail is described in Table I. The hardware processing time delay for the changing of imaginary focal point is assumed to 3 µs.

Fig. 2 describes the received power spectrum of azimuth and elevation at the RIS. The UE, RIS, and BS position are respectively set to $(3.75, 9.5, 1.47)$, $(7, 7, 5)$, and $(0, 0, 0)$, and estimated azimuth and elevation at the RIS are $31°$ and $-16°$. The power spectrum of Fig. 2 greater than azimuth $150°$ shows the spurious component, due to the phase offset from the hardware processing time delay.

V. Conclusion

This paper analyzes the performance of AoA estimation under hardware impairments and multipath propagation in RIS-assisted mmWave MIMO system. The hardware impairments are necessary to consider for the precise channel parameter estimation and sensing. Moreover, the simulated result with hardware impairments shows that spurious components are revealed.

Acknowledgment

This work was supported by the National Research Foundation of Korea(NRF) grant funded by the Korea government(MSIT) (No. NRF-2023R1A2C3002890).

References

[1] Z. Zhang *et al.*, "Active RIS vs. passive RIS: Which will prevail in 6G?" *IEEE Trans. Commun.*, vol. 71, no. 3, pp. 1707–1725, 2022.

[2] C. Pan *et al.*, "An Overview of Signal Processing Techniques for RIS/IRS-Aided Wireless Systems," *IEEE J. Sel. Topics Signal Process.*, vol. 16, no. 5, pp. 883–917, 2022.

[3] X. Mu, J. Xu, Y. Liu, and L. Hanzo, "Reconfigurable Intelligent Surface-Aided Near-Field Communications for 6G: Opportunities and Challenges," *IEEE Veh. Technol. Mag.*, vol. 19, no. 1, pp. 65–74, 2024.

[4] H. Akaike, "Information Theory and an Extension of the Maximum Likelihood Principle," in *Selected Papers of Hirotugu Akaike*. Springer, 1998, pp. 199–213.